

# SELF-ASSEMBLING ORGANIC FERROMAGNET: FRONTIER ORBITAL CONTROL OF SPIN- POLARIZED ORGANIC RADICALS

TADASHI SUGAWARA, JOTARO NAKAZAKI,  
AND MICHIO M. MATSUSHITA

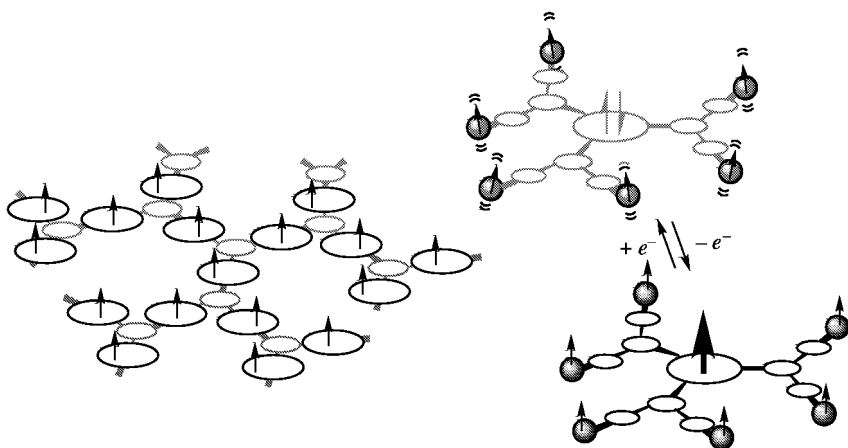
*Department of Basic Science, Graduate School of Arts and Sciences,  
The University of Tokyo 153-0089, Japan*

## PREFACE

A recent progress in synthetic methodology, such as a convergent method, a divergent one and their hybrids, enables to prepare organic giant molecules, *e.g.* dendrimers, molecular wires, bandanna molecules, *etc.*, with a molecular size of more than a few nano-meters.<sup>1</sup> Different from polymers, there is no distribution of molecular weights of such giant molecules. Furthermore, a shape of the molecular structure can be designed three-dimensionally. Such a giant molecule can be designated as a hyper-structured molecule (*HSM*). If *HSM* is composed of plural units with different functionalities, the molecule as a whole is expected to manifest integrated functions, *e.g.* a vectorial transportation of electrons or protons, or an extremely efficient light harvesting property, *etc.*, by itself just as proteins do.<sup>2</sup> These functions can hardly be achieved by conventional functional molecules or polymers. On developing a single molecular device utilizing a functionalized *HSM*, accessibility to *HSM* becomes a crucial point. Although there are still a lot of problems to be solved before being able to manipulate functionalized *HSMs*, techniques in nanotechnology, such as scanning probe microscopy, will become powerful means in this respect.

Among functional organic materials, topologically controlled high spin molecules have drawn much attention. Discovery of the quintet *meta*-phenylene-bis(phenylmethylene) by Itoh and Wasserman was followed by the generation of the ground state nonet tetracarbene of which spin quantum number exceeds those of transition metals.<sup>3</sup> Thereafter, a number of high spin polyradicals and polycarbenes have been prepared.<sup>4</sup> The fundamental issues and recent spectacular achievements related to the hyper-structured high spin molecules (Fig. I, left) are described in Volume I of this series.

Since the intrinsic character of an organic spin system is that unpaired electrons occupy  $\pi$ -orbitals, modulation of the  $\pi$ -system is expected to control the magnetic



*Hyper-Structured High Spin Molecule*      *Hyper-Structured Spin Polarized Donor*  
**Figure 1.** Hyper-structured magnetic molecules.

interaction between unpaired electrons in  $p$ -orbitals.<sup>5</sup> Along this line, a donor radical, in which a radical unit is connected with a donor unit in a cross-conjugating manner, has been explored.<sup>6</sup> When a donor unit is singly oxidized, a generated unpaired electron is coupled ferromagnetically with an unpaired electron of the radical unit. Such a type of donor radical is called *spin-polarized donor* and its potential applicability is discussed in Volume II.

Another approach to realize organic ferromagnetic materials is to self-assemble organic radicals in such a way as to exhibit ferromagnetic intermolecular interaction. In this approach, the spin multiplicity of a constituent open-shell molecule does not need to be large. The point is how to control an intermolecular magnetic interaction, which is, in most cases, anti-ferromagnetic.

The strategy for obtaining ferromagnetic molecular assembly is as follows (Fig.2). First, organic radicals with a spin-polarized electronic structure should be prepared. The spin-distribution and energy levels of  $p$ -orbitals of these radicals are largely affected by an unpaired electron on the radical unit. Next, relative orientation of spin-polarized organic radicals must be adjusted finely so as to induce a ferromagnetic intermolecular coupling. For this purpose, spin-polarized organic radicals with an orientation controlling site (*OCS*) are designed.<sup>7</sup> Then, the *OCS*-assisted self-assembly is expected to exhibit a desired magnetic property spontaneously. On evaluating the magnetic properties of the self-assembly precisely, it is a best way to use single crystals because one can elucidate a correlation between the structure and the magnetic property in detail based on the crystallographic data. Information obtained by the above methodology will be indispensable to construct integrated *HSMs* which are hopeful functional materials in the 21st century.

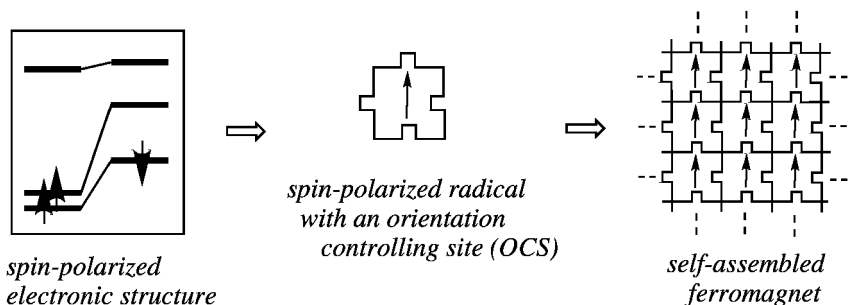


**Figure 2.** Self-assembled molecular magnetic system.

This chapter describes the spin-polarized electronic structure of organic radicals in detail, including a UHF description, and discusses the possible orbital interactions between spin-polarized UHF-orbitals. Several examples of spin-polarized organic radicals with an *OCS*, such as a long alkyl chain, an electronically polarized group, a hydrogen-bonding site, *etc.*, are introduced systematically by classifying a type of magnetic interactions and a kind of stable radical units. Finally an approach to a spin-polarized molecular wire will be proposed as a prototype of an organic quantum spin device.

## THEORETICAL STUDIES ON INTERMOLECULAR MAGNETIC INTERACTION

### Interpretation Based on McConnell's Model

An organic  $\pi$ -radical, in general, has a characteristic electronic structure. In allyl radical, for example, an  $\pi$ -spin in SOMO (singly occupied molecular orbital) distributes on  $C_1$  and  $C_3$  carbons (*spin-delocalization*), and the distribution of the  $\pi$ -spin in SOMO influences those of  $\sigma$ - and  $\pi$ -spins in NHOMO (next highest occupied molecular orbital): While the distribution of the  $\pi$ -spin in NHOMO is rather unaffected, that of the  $\sigma$ -spin tends to avoid residing on  $C_1$  and  $C_3$  (Fig.3). As a result, a negative spin density is resulted on  $C_2$ , giving rise to an alteration of the spin densities. This modulation in the spin distribution is called *spin-polarization*.

Next, let us consider the intermolecular magnetic interaction of allyl radicals in various orientations. Since the carbons carrying antiparallel spins can form a covalent bond when they come close, the local intermolecular interactions between spin-distributing carbon atoms are anti-ferromagnetic. This interaction is called

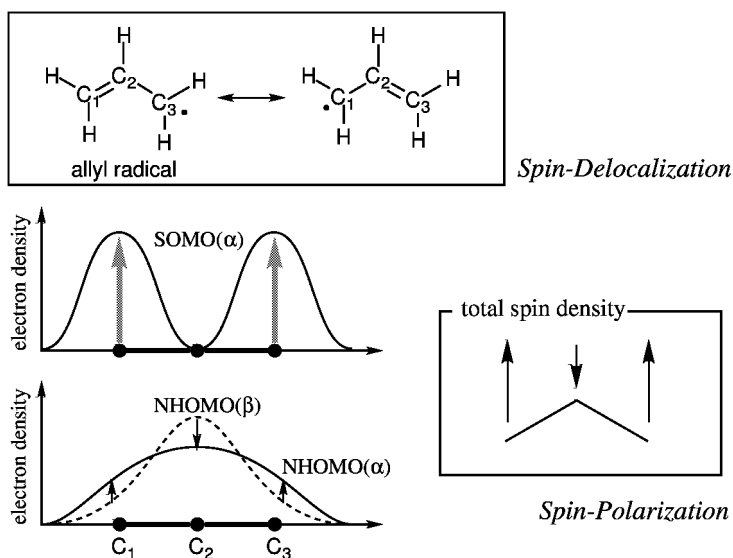


**Figure 3.** Spin-delocalization and spin-polarization in allyl radical.

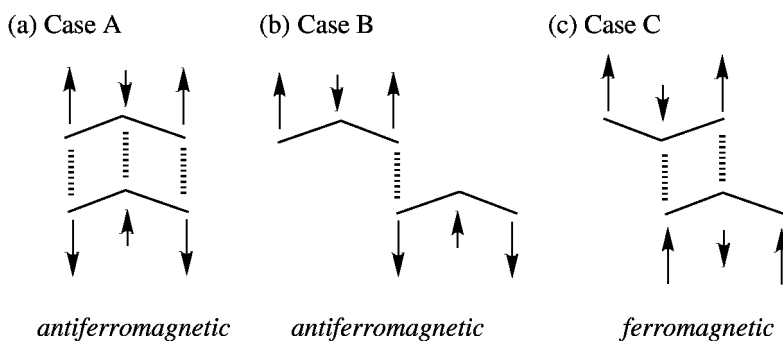


**Figure 4.** Relative orientations and intermolecular magnetic interactions of allyl radicals.

a "kinetic exchange" effect. When a pair of allyl radicals are aligned in the arrangement of (a) or (b) in Fig.4, the overall intermolecular interaction becomes anti-ferromagnetic. On the other hand, the arrangement (c) in Fig.4 leads to a net ferromagnetic interaction by the same token. Consequently, it is obvious that the intermolecular magnetic interaction depends heavily on the relative orientations of  $\cdot$ -radicals. This type of analysis on the intermolecular magnetic interaction is called McConnell's model study.<sup>8</sup>

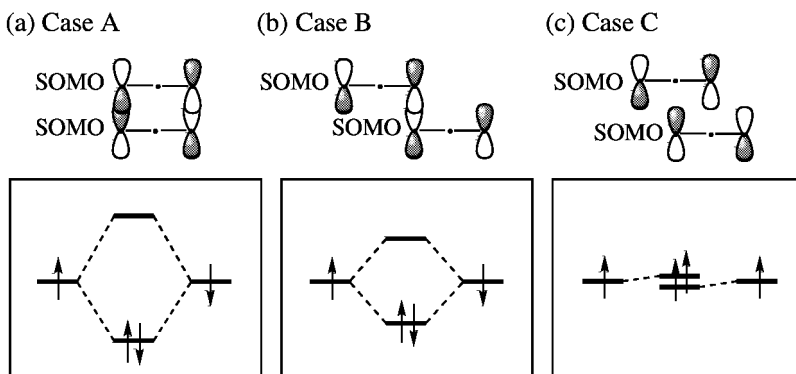


**Figure 5.** Orbital interactions between two allyl radicals in various configurations.

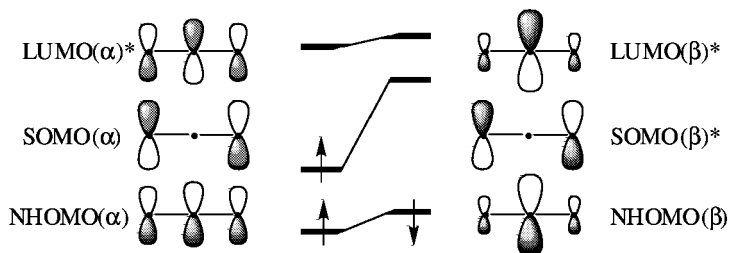
### Interpretation Based on Molecular Orbital Method

Here we consider molecular orbital interactions between two allyl radicals in three configurations (Fig.5(a)-(c)). Since the highest  $\pi$ -molecular orbital between two allyl radicals is singly occupied. Therefore, the most significant orbital interaction is between SOMOs of two allyl radicals. When two SOMOs interact in phase with a non-zero overlap integral, as shown by configurations of case A or B, two electrons of different spins occupy the lower energy orbital which is resulted from a symmetric combination of two SOMOs. While in configuration C, two SOMOs are nearly orthogonal to each other and degenerated. Two spins, therefore, occupy each SOMO separately, resulting in the triplet ground state on the basis of the exchange interaction as far as two MOs overlap effectively.

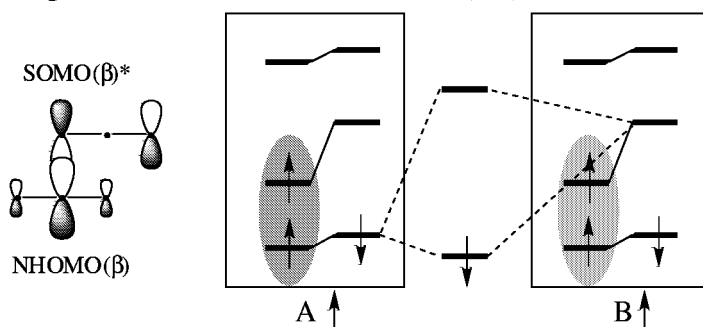
The origin of ferromagnetic interaction between allyl radicals of type C configuration can be discussed more quantitatively on the basis of a UHF description. Strictly speaking, two different electron spins in one molecular orbital in a molecular orbital don't necessarily occupy the same space, but they reside separately. Considering this situation, a UHF method provides two spins with two different UHF-MOs, *e.g.* NHOMO( ), NHOMO( ). First, we will consider the spin-distribution and orbital energies of an isolated allyl radical. Fig.6(a) shows the energy level and the shape of UHF orbitals of an allyl radical schematically. When SOMO( ) interacts with NHOMO( ), the coefficient at  $C_2$  carbon of NHOMO( ) increases and its energy level is destabilized. On the other hand, the coefficients and the energy level of NHOMO( ) are relatively unaffected because two spins in SOMO( ) and NHOMO( ) never come close to each other based on Pauli's exclusion principle.

Next, let us consider the intermolecular orbital interaction of the type C. Since two SOMOs are nearly orthogonal to each other, NHOMO-SOMO\* (asterisk

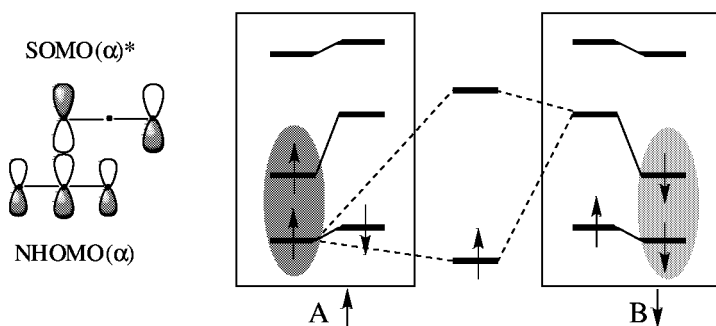
## (a) Molecular orbitals of allyl radical in UHF description



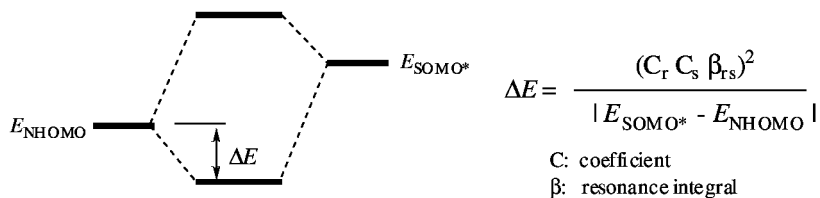
## (b) Ferromagnetic UHF orbital interaction / Case C(FM)



## (c) Antiferromagnetic UHF orbital interaction / Case C(AFM)



## (d) Energy diagram of orbital interaction


**Figure 6.** UHF description of orbital interactions between two allyl radicals.

represents a vacant orbital) interaction becomes influential in the magnetic interaction.

Here arises a question regarding which is more stable, case C(FM) or case C(AFM) (Fig.6(b) or Fig.6(c)). As far as the energetic term is concerned, the orbital energy of  $\text{NHOMO}(\sigma)$  is lower than that of  $\text{NHOMO}(\pi)$ . Therefore, the energy difference between  $\text{NHOMO}(\sigma)$  and  $\text{SOMO}(\sigma)^*$  ( $E_{\text{SOMO}(\sigma)^*} - E_{\text{NHOMO}(\sigma)}$ ) is smaller than that between  $\text{NHOMO}(\sigma)$  and  $\text{SOMO}(\pi)^*$  ( $E_{\text{SOMO}(\pi)^*} - E_{\text{NHOMO}(\sigma)}$ ). Moreover, the orbital overlap between  $\text{NHOMO}(\sigma)$  and  $\text{SOMO}(\sigma)^*$  (Fig.6(b)) is larger than  $\text{NHOMO}(\sigma)$  and  $\text{SOMO}(\pi)^*$  (Fig.6(c)) because of the larger coefficient at  $\text{C}_2$  carbon atom in  $\text{NHOMO}(\sigma)$ . Accordingly, the ferromagnetic interaction (Fig.6(b)) predominates over the anti-ferromagnetic one (Fig.6(c)) according to the perturbational interaction as depicted in Fig.6(d).

### Experimental Model for Intermolecular Magnetic Interaction

Significance of a relative orientation of organic radicals regarding to the intermolecular magnetic interaction can be clearly demonstrated using benzyl radical as a model for organic  $\pi$ -radicals containing a spin-distributing aromatic ring (McConnell's rule). As shown in Fig.7(a), the coefficients of benzyl radical distribute only at *ortho* and *para* positions, beside the largest coefficient at the benzylic carbon atom. Suppose that two phenyl rings are overlapped, a series of orientations of two benzyl radicals are depicted in Fig.7(b)-(e). In the case where the twist angle ( $\theta$ ) in reference to the rotation axis is  $60^\circ$  or  $180^\circ$ , the overlap integral between two SOMOs is negligibly small and two orbitals are almost orthogonal to each other. The intermolecular magnetic interaction, therefore, is ferromagnetic in these orientations (Fig.7(c),(e)). Whereas in

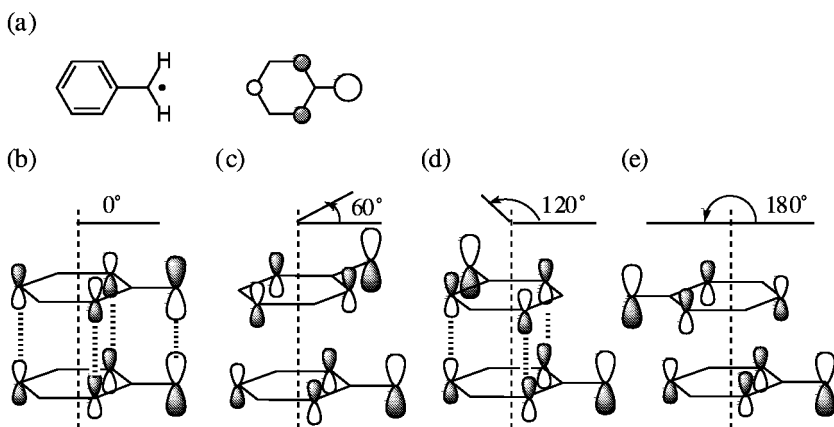


**Figure 7.** Orbital interactions between two benzyl radicals in various configurations.

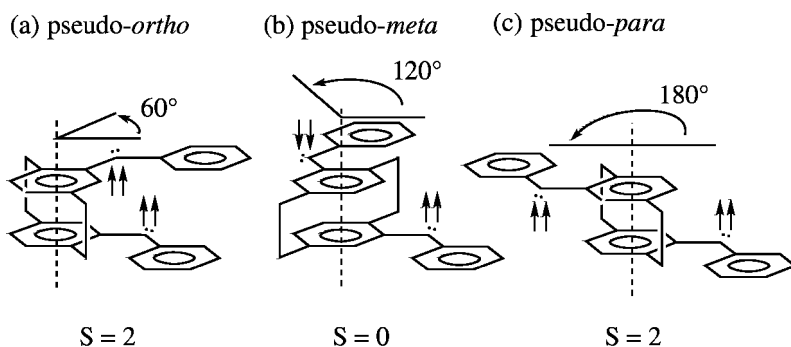


**Figure 8.** Magnetic interactions in cyclophanedicarbene with various mutual orientations.

orientation with the twist angle of  $0^\circ$  or  $120^\circ$ , the overlap integral is significantly large, leading to the anti-ferromagnetic interaction (Fig.7(b),(d)).

The isomeric [2.2]paracyclophane-dicarbene were generated photochemically from the corresponding bis(diazo) compounds which are model compounds to examine the ferromagnetic intermolecular magnetic interaction (Fig.8).<sup>10</sup> The ESR spectra of the *pseudo-ortho* ( $= 60^\circ$ ) and *pseudo-para* isomers ( $= 180^\circ$ ) show intense ground state quintet signals due to the ferromagnetic coupling ( $E_{QT} = 0.18, 0.31$  kcal/mol), while the *pseudo-meta* isomer gives a thermally populated triplet signal, indicating that this isomer has the singlet ground state due to the anti-ferromagnetic coupling ( $E_{ST} = 0.28$  kcal/mol). This is clear experimental evidence for the McConnell's rule concerning the intermolecular spin alignment.

### Intermolecular Interaction in Cluster of Diphenylcarbenes

The magnetic interaction within cluster of diphenylcarbenes, generated photochemically in the host crystal of the corresponding diazo precursor, was found to be well rationalized in terms of the crystal structure of the host diazo compound.<sup>10</sup> An ESR spectrum of photolyzed bis(4-methoxyphenyl) diazomethane consists mainly of intense quintet (Q) signal, which is assignable to a ferromagnetically coupled carbene pair. Such an interaction seems to be achieved by the dimeric crystal structure of the parent diazo compounds, taking a *pseudo-para* type orientation (Fig.9(a)). On the other hand, the magnetic interaction in the cluster of bis(4-chlorophenyl)methylene generated in the crystals of the corresponding diazo compounds is interpreted by the anti-ferromagnetic interaction (Fig.9(b)). Because diazo molecules in the crystal of bis(4-chlorophenyl)diazomethane are stacked in a column and benzene rings are overlapped, constituting a *pseudo-geminal* type orientation. The observed tendency is in accord with the anti-ferromagnetic interaction predicted.



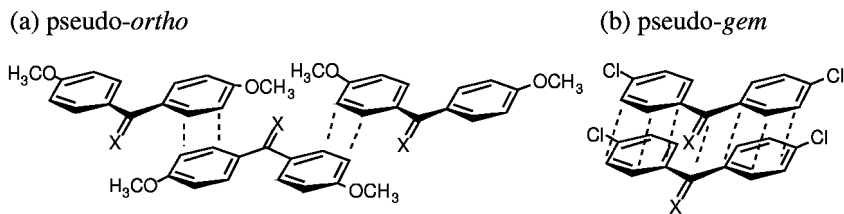


**Figure 9.** Magnetic interactions in diphenylcarbene derivatives ( $X = N_2$  or  $\bullet\bullet$ ) in host crystals of corresponding diazo compounds.

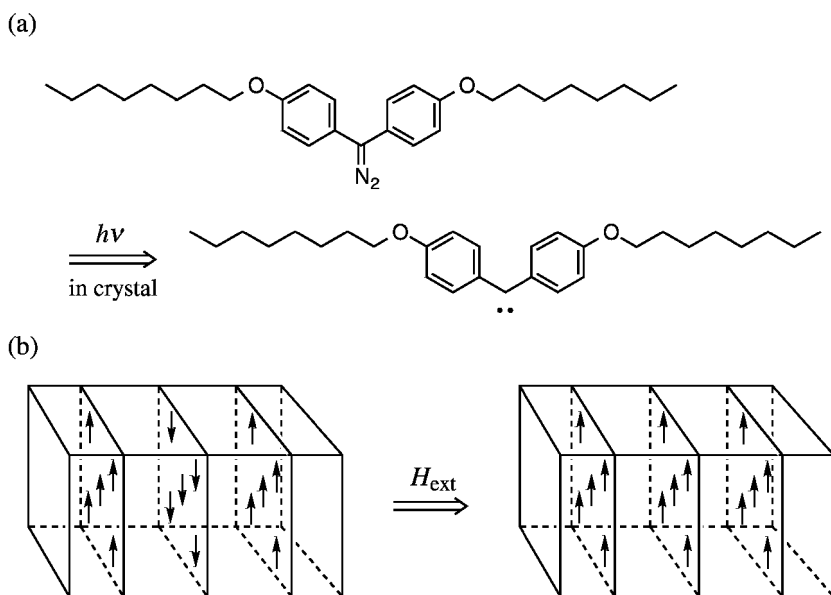


**Figure 10.** (a) Photolytic generation of bis[*p*-(octyloxy)phenyl]carbene, (b) Schematic drawings of meta-magnetic system.

In the case of bis[*p*-(octyloxy)phenyl]diazomethane, in particular, the photolyzed sample shows a positive Weiss temperature of 2 K.<sup>11</sup> Introduction of long alkyl chains at the *para*-positions of aryl diazo compounds leads to a favorable arrangement which causes a two-dimensional ferromagnetic coupling among spin-distributing benzene rings of the generated diarylcarbenes. As a result, this carbene cluster affords a two-dimensional meta-magnetic spin system (Fig.10).

## CRYSTAL ENGINEERING OF ORGANIC RADICAL CRYSTALS

## Self-Assembling Organic Radicals in Aid of Orientation Controlling Site

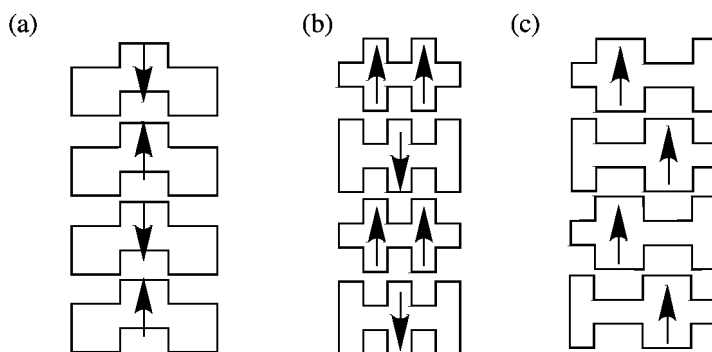


**Figure 11.** Self-assembling organic radicals with various magnetic interactions: (a) antiferro-, (b) ferri-, and (c) ferromagnetic interaction.

As described in the previous sections, the intermolecular magnetic interaction depends heavily on the relative orientation in a molecular assembly of  $\cdot$ -radicals. Under such circumstances, it is of great significance to regulate crystal structures of stable organic radicals so as to exhibit desirable magnetic properties (Fig.11). A method of controlling the crystal structure of organic radicals in aid of an *orientation controlling site (OCS)* will be proposed here. An *OCS* is a functional group which plays a significant role of self-assembling organic radicals by means of intermolecular interactions, such as electrostatic interactions, hydrogen bonds, or charge transfer interactions, *etc.* Organic radicals, then, self-assemble by themselves as paramagnetic building blocks to create a highly ordered molecular architecture of intriguing magnetic properties.

The observed magnetic properties of the radical crystals are, then, interpreted in terms of the frontier orbital interactions between spin-polarized organic radicals, while the spin-polarization mechanism is also applied to rationalize the local magnetic interaction. The latter explanation can also be rationalized by the molecular orbital interaction analysis when molecular orbitals which have significant coefficients at the locally interacting sites are taken into consideration, although those orbitals are not necessarily frontier orbitals.

### Antiferromagnetic Crystal of Diaryl Nitroxide with Long Alkyl Chains

The crystal structure and magnetic susceptibility of the crystal of bis(*p*-methoxyphenyl)nitroxide was studied extensively, and the crystal was found to exhibit a negative Weiss temperature of  $-3.4$  K.<sup>12</sup> When the decyloxy chains were introduced at the *para* positions of the phenyl rings, the absolute value of the negative Weiss temperature of the crystal was increased ( $= -10$  K) (Fig.12).<sup>13</sup>

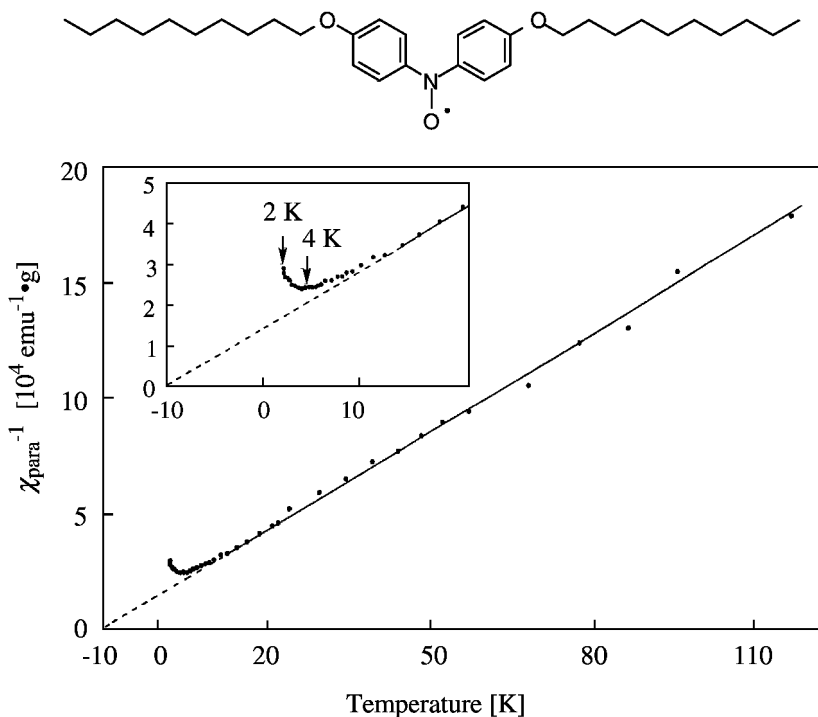


**Figure 12.** Temperature dependence of the reciprocal paramagnetic susceptibility of bis(*p*-decyloxyphenyl)nitroxide.

The enhanced anti-ferromagnetic intermolecular interaction may be due to the presence of long alkyl chains, and the dispersion force of the alkyl chain enforces a tight packing on the nitroxide molecules. The magnetic interaction of this crystal corresponds to the case which is schematically depicted by Fig.11(a).

When the field dependence of the magnetic susceptibility was measured at 2K, at higher external magnetic fields than 5 Tesla, the magnetic susceptibility was found to show an up-ward deviation from the extrapolated curve derived from the data at lower magnetic fields. This interesting phenomenon is interpreted in terms of a spin-flop mechanism which happens between the anti-ferromagnetically coupled spins. The result provides a direct proof for the presence of the antiferromagnetic coupling among neighboring nitroxide molecules.

Although the crystal structure of the nitroxide with decyloxy chains is similar to that of bis[*p*-(ocylloxy)phenyl] diazomethane, the magnetic interaction in nitroxides turned out to be antiferromagnetic. Since the spin density in the nitroxide is localized at the NO group and that only small spin densities are

distributed on the phenyl ring, the magnetic interaction between nitroxides is of an one-centered character, leading to the anti-ferromagnetic interaction.

### Crystal Engineering Organic Ferrimagnet

Even though the intermolecular magnetic interaction is anti-ferromagnetic, one can construct a ferrimagnetic system by utilizing a ground state triplet diradical and a doublet monoradical. A crystal designing ferrimagnet is, in fact,

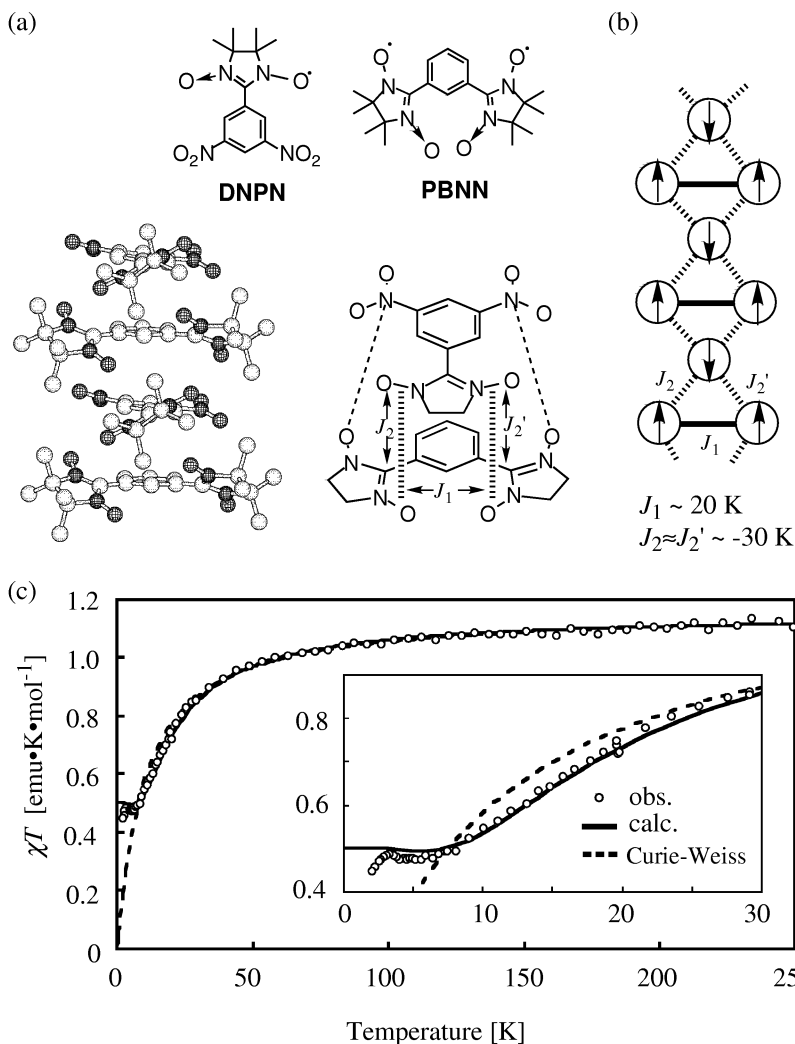


**Figure 13.** Self-assembled ferrimagnetic system.

one of the successful examples of the crystal engineering technique using OCS groups (Fig.11(b)).<sup>14</sup> As a ground state triplet diradical, *m*-phenylenebis(nitronyl nitroxide) (**PBNN**) was selected, and for a monoradical, *m*-dinitrophenyl nitronyl nitroxide (**DNPN**), where the two nitro groups on the phenyl ring of **DNPN** exert as *OCS*s. As a result of the electrostatic interaction between the nitro groups of the monoradical and the nitronyl nitroxide groups of the diradical, they are stacked alternately to form a columnar structure (Fig.13(a)). The obtained organic ferrimagnetic spin system is unique from the view point of the competing magnetic interactions between the intramolecular ferromagnetic coupling ( $J_1$ ) and the intermolecular antiferromagnetic ones ( $J_2 \sim J_2'$ ) of the same order (Fig.13(b)). The temperature dependence of the magnetic susceptibility is reproduced by diagonalization of the Heisenberg Hamiltonian for a six-spin configuration with a periodic boundary condition. The lack of the ferrimagnetic phase transition of the above crystal is argued in reference to the non-equivalent antiferromagnetic couplings ( $J_2 \sim J_2'$ ) between the two kinds of radical centers.

### Ferromagnetic Crystals of Nitroxides

Magnetic interaction in more than one hundred crystals of TMPO (2,2,6,6-tetramethylpiperidin-1-yloxy) derivatives has been investigated precisely by Nogami *et al.*<sup>15</sup> The origin of an intermolecular ferromagnetic interaction is arisen from the spin-polarization generated within an open-shell molecule. In the case of nitroxide crystals, the spin-polarization is caused not only through the  $\pi$ - $\pi$  interaction, but also through the  $\sigma$ - $\sigma$  type (hyper-conjugative) interaction. For instance, the carbon atom of the methyl group at the  $\alpha$  position to the NO group is spin-polarized positively through a hyper-conjugative mechanism (Fig.14). Accordingly, all the methyl hydrogen atoms are negatively spin-polarized. As a result, when these hydrogens are located in the proximity to the nitroxide group of the adjacent molecule, carrying with a positive spin-density,

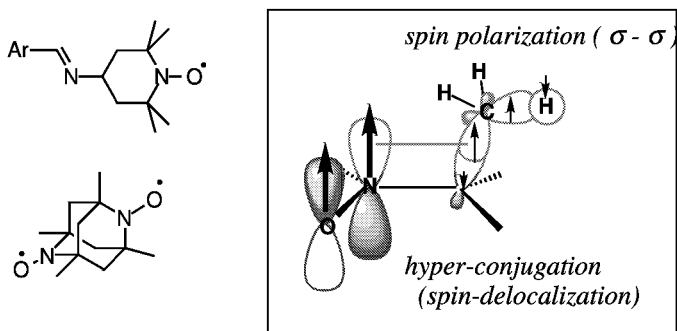


**Figure 14.** Spin-polarization in TMPO-type nitroxide radical.

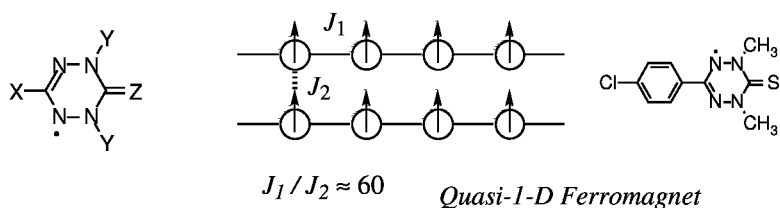


**Figure 15.** Quasi 1-D ferromagnetic spin system constructed by verdazyl radical.

the intermolecular interaction becomes ferromagnetic. This is the reason why the ferromagnetic interaction is frequently observed in crystals of nitroxide derivatives, corresponding to the case of Fig.11(c).

Spin alignment in tetramethyldiazaadamantanedioxy studied by Rassat *et al.* can be interpreted by the same mechanism.<sup>16</sup> In this case, all the hydrogen atoms of diazaadamantane skeleton are equivalent and negatively spin-polarized. Moreover, there are two ferromagnetically coupled nitroxide groups in the skeleton. The intermolecular ferromagnetic interaction is, therefore, considered to be enhanced. This may be the reason for the highest transition temperature (1.48 K) of this crystal among genuine organic ferromagnets so far reported.

### Ferromagnetic Crystals of Verdazyls

Various verdazyl derivatives have been prepared, and a number of organic ferromagnets, ferrimagnets, meta-magnets have been developed based on the crystals of verdazyl derivatives.<sup>17</sup> The probability of affording ferromagnetic crystals is as high as that of nitronyl nitroxide crystals (See, the following section). The characteristic electronic structure plays a crucial role in manifesting an intermolecular ferromagnetic interaction. Namely, SOMO of a verdazyl radical has  $C_{2v}$  symmetry and the energy level of SOMO is located underneath of HOMO as in the case of nitronyl nitroxides. The difference in the magnetic interaction between verdazyl radicals and nitronyl nitroxides is that a lack of the transmitting route of magnetic interaction other than  $\pi$ -type interactions in the former: Most of verdazyl radicals do not carry  $\pi$ -methyl groups of which hydrogen atoms are negatively spin-polarized. This structural feature strengthens the intermolecular magnetic interaction of the  $\pi$ -type, but at the same time the dimensionality of the magnetic interaction is likely to become low-dimensional (Fig.15).

## FERROMAGNETIC CRYSTALS OF ARYL NITRONYL NITROXIDES

### Electronic Structure of Phenyl Nitronyl Nitroxide

Before discussing a spin-polarized electronic structure of aryl nitronyl

nitroxides in terms of a UHF-MO description, it is worth-while to sketch its characteristic electronic structure according to a perturbational molecular orbital approximation (PMO-RHF). The features of frontier orbitals represented by PMO description can be pointed out as follows (Fig.16). First, one will notice that the coefficients of SOMO of phenyl nitronyl nitroxide (**PhNN**) are restricted only on the nitronyl nitroxide (NN) group. Whereas *somo* of the NN group has  $a_2$  symmetry due to the presence of a  $C_2$  symmetry axis, the symmetry of the partial molecular orbital of the aryl substituent is not necessarily  $a_2$ . Thus *somo* of the NN group becomes SOMO of the entire molecule without being perturbed. Even though the symmetry of two units, the NN group and the substituent, coincides, the perturbation between two units should be subtle, because the coefficient at  $C_2$  of *somo* of the NN group is negligibly small. Second, contrasting to SOMO, the coefficients of NHOMO of **PhNN** spread over to the entire molecule as a result of the interaction between *homo* of benzene and *nhomo* of the NN group. On the other hand, LUMO of **PhNN** is resulted from the interaction between *lumo* of benzene and *lumo* of the NN group. The above tendency in the shapes of frontier orbitals can be seen commonly in most of NN derivatives. The exception is the case where the NN group is severely twisted from the plane of the rest of the molecule.

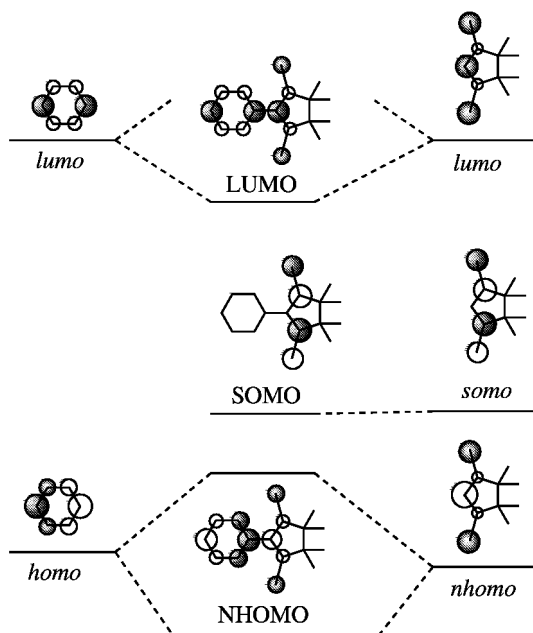


**Figure 16.** Perturbational MO description of phenyl nitronyl nitroxide.

### Orbital Interaction between Spin-Polarized Aryl Nitronyl Nitroxides

In this section, one will examine three types of intermolecular frontier orbital interactions of organic radicals, in which electrons in NHOMO is spin-polarized by an unpaired electron in SOMO( ) (Fig.17). Since the highest UHF-MO is SOMO( ) in case I, the predominant interaction is between SOMO( ) of molecule A and SOMO( )\* of molecule B. This SOMO-SOMO\* interaction leads to an antiferromagnetic intermolecular interaction. In case II, the NN unit interacts with the aryl unit not with the NN unit of the adjacent molecule, *vice versa*. Furthermore, the spin polarization is significantly large, and the energy level of NHOMO( ) is higher than SOMO( ): This type of a spin-polarized radical can be designated as a spin-polarized donor. The crucial interaction is, therefore, between NHOMO( ) and SOMO( )\*, giving rise to a ferromagnetic interaction: In case III, The NN unit interacts with the aryl unit predominantly as in the case II. Since the energy level of LUMO( ) is lower than that of SOMO( )\*,

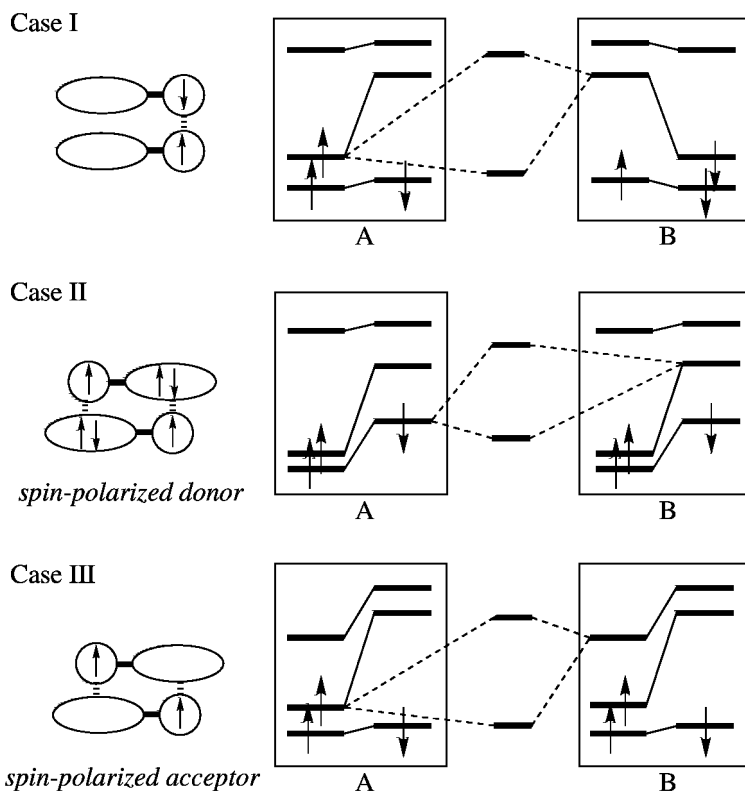


**Figure 17.** Schematic drawings of UHF orbital interactions between three types of organic radicals.



SOMO( ) and LUMO( ) interact predominantly to lead also to a ferromagnetic interaction: Such a type of radical is called spin-polarized acceptor.

Taking account of these orbital interaction, one can design a spin-polarized electronic structure such as case II or III by introducing electron-releasing or electron-withdrawing substituent into the aromatic ring, respectively. These spin-polarized radicals have a chance to realize an organic ferromagnet when they are assembled properly. The concrete examples will be described in the subsequent sections.

### Organic Ferromagnet Composed of Spin-Polarized Acceptor : *p*-Nitrophenyl Nitronyl Nitroxide (*p*-NPNN)

*p*-Nitrophenyl Nitronyl Nitroxide (*p*-NPNN) is the first genuine organic ferromagnet, and it affords four crystal phases, including the  $\beta$ -phase which exhibits a ferromagnetic phase transition.<sup>18</sup> The molecular arrangements in these phases are different, but the ferromagnetic interaction is observed in all four phases. This tendency suggests that the electronic structure of *p*-NPNN itself contributes

to the appearance of the ferromagnetic interaction.

An energy diagram of the electronic structure of *p*-NPNN is calculated by a semiempirical MO (MOPAC-PM3/UHF) method. As shown in Fig.18, the highest MO is SOMO( ) as in the case of regular organic radicals. The energy level of SOMO( ) is, however, not the lowest unoccupied orbital, but LUMO( ) is the lowest. This electronic structure is caused by an electron-withdrawing nitro group at the *para*-position of the aromatic ring, corresponding to case III in Fig.17.

The magnetic interaction in *p*-NPNN was, in particular, elucidated precisely by means of magnetic susceptibility, heat capacity,  $\mu$ SR, and neutron diffraction experiments.<sup>19</sup>

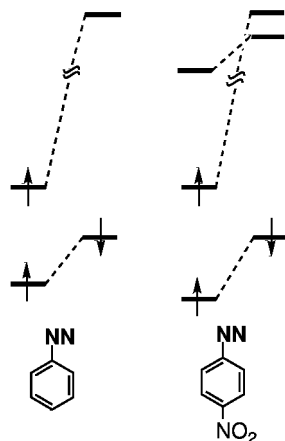


**Figure 18.** Molecular orbitals of phenylNN and *p*-NPNN.

### Experimental Support for Electronic Structure of Spin-Polarized Acceptor

*p*-Benzoquinone nitronyl nitroxide (**BQNN**) consists of nitronyl nitroxide (NN) and benzoquinone (BQ) units, the latter of which is a reasonably good acceptor. The symmetry and the energy level of SOMO of **BQNN** is practically the same as those of phenyl nitronyl nitroxide (Fig.19). On the other hand, coefficients of LUMO spread over to the entire molecule, indicating that LUMO is resulted

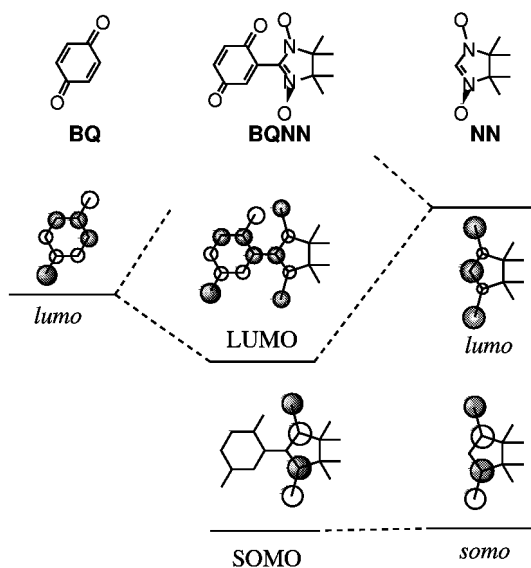


**Figure 19.** Perturbational MO description of BQNN.

from the interaction between *lumos* of both units (BQ and NN). Accordingly, the energy level of LUMO is lowered compared with that of BQ. The above calculated result on **BQNN** was supported with the electrochemical data. Namely, the reduction potential of **BQNN** (-0.23 V) is lower than that of BQ (-0.44 V). It is to be noted that the orbital by which an electron is accepted is LUMO( ) in the UHF description as in the case of *p*-NPNN. This suggests that **BQNN** should afford an anion radical of a ground state triplet spin multiplicity by one-electron reduction. **BQNN** was, indeed, found to afford a ground state triplet ESR signal, when it was reduced by sodium in dimethylformamide (DMF) solution.<sup>20</sup> This experimental result is a strong support for the calculated electronic structure of **BQNN**.

From the temperature dependence of the magnetic susceptibility of the polycrystalline sample of **BQNN**, more than six spins at average are coupled ferromagnetically at 4 K. In the crystal, **BQNN** molecules are stacked to form a one-dimensional column, although two modes of overlap are involved in the column. While a ferromagnetic interaction is predicted for one of the overlapping modes, the other is not necessarily ferromagnetic. In spite of this inhomogeneity in magnetic interactions, the magnetic data was found to be reproduced by a quasi-one-dimensional ferromagnetic model with  $J = 15$  K and  $J' = -0.12$  K (Fig.20). The observed ferromagnetic interaction along the one-dimensional chain cannot be rationalized merely by the mutual orientation of spin-containing molecules, but may be understood by the intrinsic contribution of the characteristic electronic structure of **BQNN** as a spin-polarized acceptor.

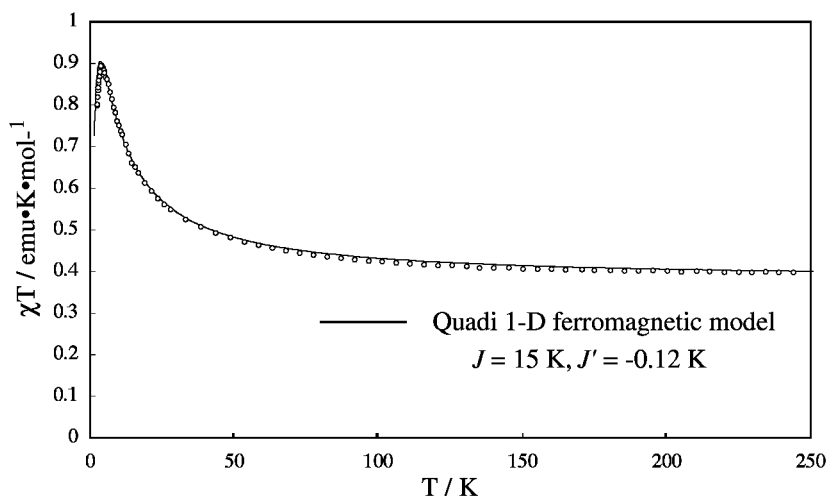


**Figure 20.** Temperature dependence of magnetic susceptibility of BQNN.

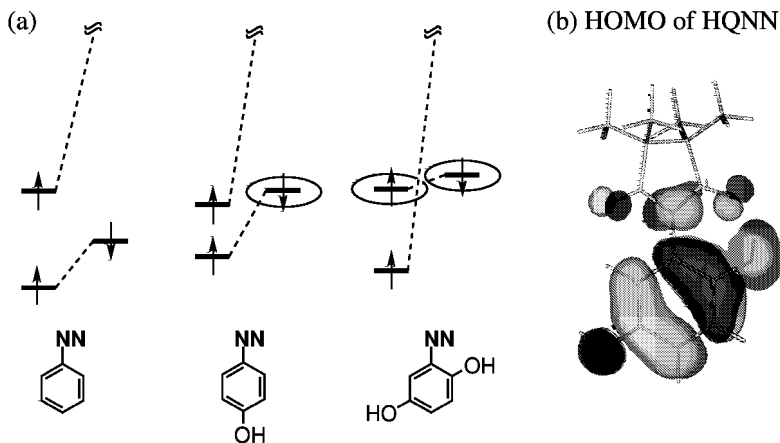


**Figure 21.** Molecular orbitals of hydroxyphenylNNs.

### Hydrogen-Bonded Organic Ferromagnet Composed of Spin-Polarized Donor

As described in the previous section, *p*-NPNN, which gives birth to the first organic ferromagnet, carries an electro-withdrawing substituent, and its spin-polarized electronic structure is classified as case III in Fig.17. It is worthwhile to prepare an aryl NN derivative with an electro-releasing group. Among electro-releasing substituents, a hydroxy group, in particular, is interesting, because a phenolic derivative is expected form a hydrogen bond with a nitronyl nitroxide group. When a hydroxy group is introduced to *ortho* or *para* position of phenyl

nitronyl nitroxide, HOMO( ) is located above SOMO( ) (Fig.21).

In di-substituted derivatives, both HOMO( ) and ( ) tuned out to be located above SOMO( ), corresponding to case II in Fig.17. Consequently, several phenol derivatives carrying a nitronyl nitroxide group were designed and prepared. Among them, hydroquinone nitronyl nitroxide (**HQNN**) has become one of the most well characterized organic ferromagnets.<sup>21</sup>

As an example, 2,6-di-*tert*-butyl-4-NN-phenol was found to afford a phenoxy radical when the precursor was oxidized under a basic condition.<sup>22</sup> This phenoxy radical was isolated as a solid and the magnetic susceptibility measurement proved a triplet ground state of the diradical. Interestingly, the ferromagnetic coupling turned out to be larger than 300 K ( $J > 300$  K). The experimental result is consistent with the spin-polarized structure of the donor radical. It is to be noted, however a sophisticated calculation places NHOMO( ) under SOMO( ), although HOMO( ) is located above SOMO( ) when the phenolate anion is generated. The PM3 method turned out to overestimate the spin-polarization in this case. The strong ferromagnetic coupling is originated from the space-sharing nature of *somo*, which is localized on NN, and *somo'*, which is generated from HOMO upon one-electron oxidation, is delocalized over the diradical molecule.

### Magneto-Structural Correlation in Hydroquinone Nitronyl Nitroxide (**HQNN**)

**HQNN** was found to afford two phases of crystals. In the  $\beta$ -phase crystal, in particular, the phenolic hydroxy group at the *ortho*-position not only forms a strong *intramolecular* hydrogen bond with the nitroxide group (O...O distance of 2.51 Å), but also forms an *intermolecular* hydrogen bond with the nitroxide oxygen of the facing **HQNN** (Fig.22(a)). This hydrogen-bonded dimer also participates in *intermolecular* hydrogen bonds with the hydroxy groups at the *meta*-position of the translated molecules with a distance of 2.75 Å. The two parallel hydrogen-bonded chains of **HQNN** run along the *c*-axis with the symmetry of inversion between facing molecules. These doubly hydrogen-bonded chains are arranged in a herringbone-type structure as depicted in Fig.22(b). It is also to be noted that the oxygen atom of the NN group is closely located to a hydrogen atom (2.74 Å) of the methyl group of **HQNN** in the neighboring chain.

The magnetic susceptibility of the polycrystalline sample of **HQNN** was analyzed by the S-T model ( $J/k_B = 0.95$  K) with a positive Weiss temperature of  $\theta = +0.44$  K. The ac susceptibility of **HQNN** increased rapidly at around 0.5 K, suggesting that a phase transition to the ferromagnetic phase occurred at this temperature (Fig.23(a)). Since the estimated saturation value of the magnetization was very close to the theoretical one ( $1 \mu_B \cdot \text{mol}^{-1}$ ), the phase transition could be regarded as a bulk transition. The crystal shows a hysteretic behavior, although

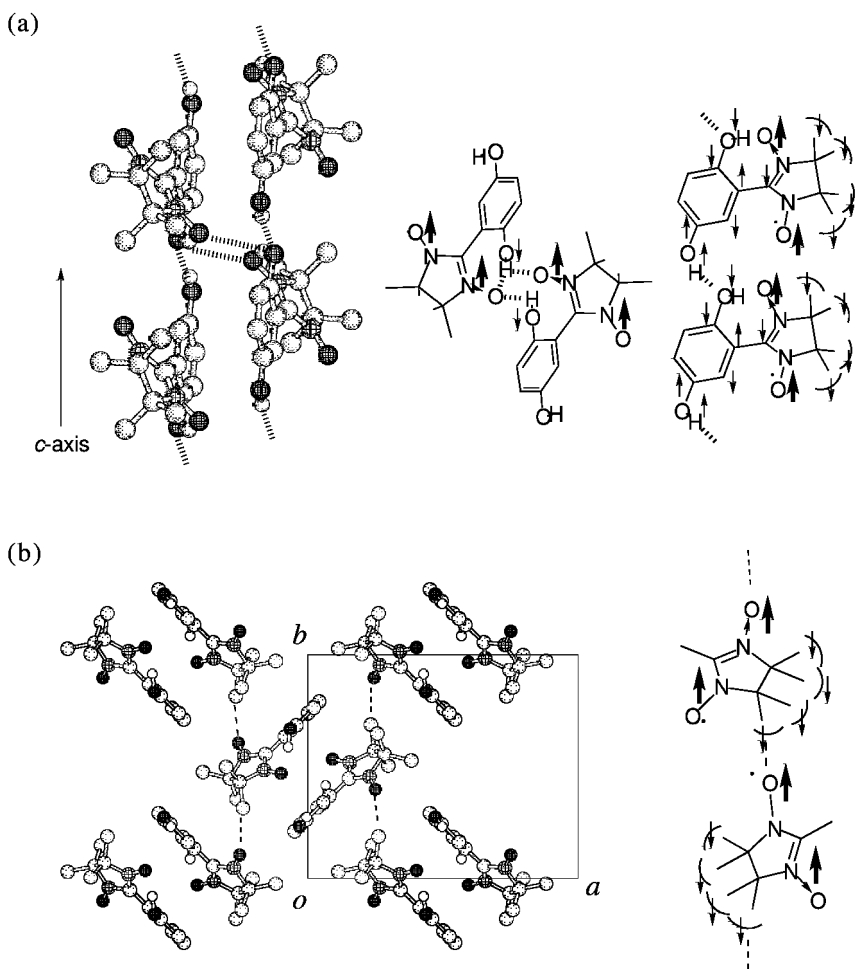


**Figure 22.** Crystal structure of HQNN. The spin-polarization at the intermolecularly interacting sites are also shown.

a coercive force was less than 20 Oe. From the heat capacity data, the spin system of **HQNN** turns out to be expressed by the three-dimensional Heisenberg model with a number of the nearest neighbors of  $z = 6$  (Fig.23(b)).

The magnetic property of **HQNN** was found to be consistent with the crystal structure as discussed above. First, the dimeric ferromagnetic coupling can be assigned to the hydrogen-bonded face-to-face dimer between the *o*-hydroxy groups which are negatively spin-polarized and the oxygen atoms of NN which are, in turn, positively spin-polarized. Second, the spin polarization should be transmitted ferromagnetically along the one-dimensional hydrogen-bonded chain, because

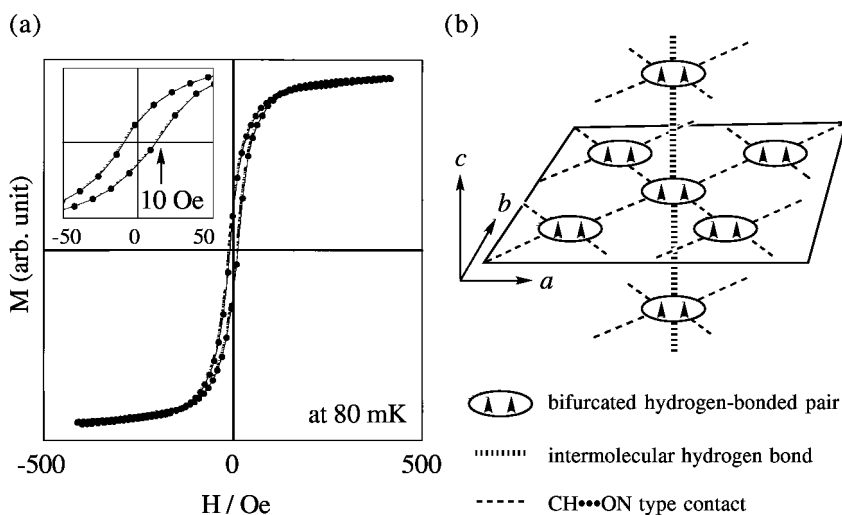


**Figure 23.** (a) Hysteretic magnetization curve of HQNN. (b) Three dimensional spin system of HQNN.

the signs of the spin densities of these sites are opposite. The ferromagnetic interaction along this direction is considered to be strengthened, because the nitronyl nitroxide group is close to the negatively spin-polarized methyl hydrogen of the neighboring molecule. Third, the  $\text{CH}\cdots\text{ON}$  interaction also exists in the  $ab$  plane and it should increase the dimensionality of the ferromagnetic interactions in the crystal.

The maximum of the heat capacity, which indicates ferromagnetic phase-transition, was shifted to the lower temperature side when the phenol groups were deuterated ( $\text{HQNN-d}_2$ ). This is a proof for the role of hydrogen-bond for the intermolecular transmission of the spin-polarization. Furthermore, the temperature dependence of the chemical shift of the deuterioxy group of  $\text{HQNN-d}_2$  in the solid state  $^2\text{H-NMR}$  spectrum indicates that the negative spin is polarized on the deuteron of the deuterioxy group.<sup>23</sup> Intermolecular magnetic coupling in the crystal of  $\text{HQNN}$  was also investigated by the sophisticated MO technique using a dimeric cluster model.<sup>24</sup> The calculated result revealed the intrinsic contribution of the hydrogen-bond to the ferromagnetic coupling. Judging from these experimental and theoretical results, it may be concluded that the hydrogen-bonds in  $\text{HQNN}$  crystal play an intrinsic role for the intermolecular transmission of the spin-polarization.

## Molecular and Crystal Design for Organic Ferromagnetic Metal

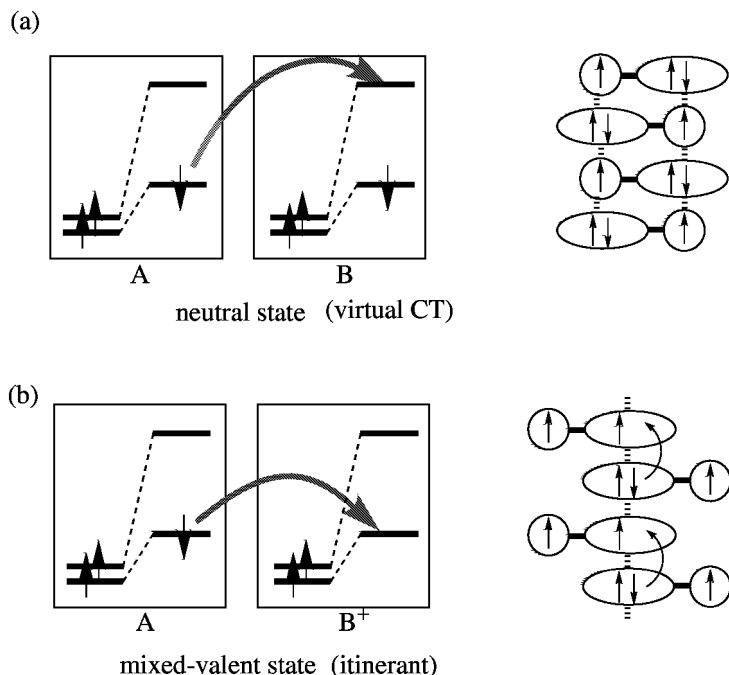


**Figure 24.** Orbital interactions of spin-polarized donor in neutral and mixed-valent state.

Although a number of organic ferromagnets have been discovered, the transition temperatures to the ferromagnetic state are still low.<sup>25</sup> In order to introduce much larger ferromagnetic interactions into an assembly of organic radicals, it is effective to use conduction electrons as a transmitter of the spin-polarization.<sup>26</sup> For this purpose, a TTF-based spin-polarized donor, which affords a ground state triplet cation diradical upon one-electron oxidation, may become an important building block for constructing a conducting magnetic material. Such a spin-polarized donor should exhibit the intermolecular orbital interaction of case II type based on the intermolecular HOMO( )-SOMO( )\* interaction in the neutral state. Since the on-site Coulomb ( $U$ ) of HOMO of a TTF skeleton is small, the electron in HOMO is expected to show itineracy when the mixed valent state is realized in the donor radical column (Fig.24). Thus the spin-alignment of the unpaired electron in SOMO( ) is guaranteed by the spin-polarized ( ) conduction electrons.

As a prototypical donor-radical, a TTF derivative carrying a nitronyl nitroxide group (**TTF-NN**) was prepared (Fig.25).<sup>27</sup> Although a triplet ESR spectrum was observed in an iodine-doped sample of **TTF-NN**, the triplet signal was found to be a thermally populated one ( $J = -100$  K). The result was attributed to the

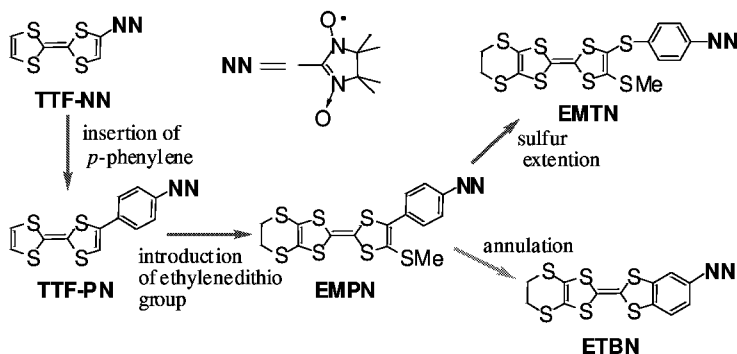


**Figure 25.** TTF-based spin-polarized donors.

twisting around a C-C bond between of the NN group from the TTF plane. In order to remove such a steric repulsion, a *p*-phenylene group was inserted between the donor site and the radical site. The modified donor radical, **TTF-PN**, afforded a ground state triplet cation diradical (**TTF-PN<sup>+</sup>**) upon one-electron oxidation. Furthermore, sulfur-extended derivatives, **EMPN** and **EMTN**, were prepared in order to enhance the kinetic stability and to increase the intermolecular interaction.<sup>28</sup> Although these donors afforded triplet cation radicals (**EMPN<sup>+</sup>** and **EMTN<sup>+</sup>**) of a reasonably high stability, no crystalline ion-radical salts were obtained.

A benzo-annulated derivative, **ETBN**, was found to show good crystallinity, and it gave birth to single crystals of a neutral donor.<sup>29</sup> In the crystal The arrangement of donor molecules are related with rotatory inversion axes (space group:  $R\bar{3}$ ), and the crystal exhibits a ferromagnetic intermolecular interaction ( $\theta \sim +0.5$  K). This novel donor was found to give crystalline ion-radical salts of the 2:1 donor to counter-ion ratio through a galvanostatic electrocrystallization. The salt exhibited both conductivity and magnetism: The salt was a semiconductor ( $E_a = 0.16$  eV) with a room temperature conductivity of  $10^{-2}$  S/cm. At the same time, the salt showed a paramagnetic behavior with a Curie constant of 0.73 emu/mol at room temperature, indicating that all the radical sites remained intact during the electro-crystallization. Although the  $\pi$ -spins on the donor sites are conductive, the density of the charge carrier is still very low in this salt, so that the spin polarization of the  $\pi$ -spin caused by the local spin on the radical site can not be transmitted to the neighboring local spins. The above result, however, promises that magnetic ordering of the local spins may be observed, if the carrier concentration in the ion-radical salt becomes reasonably high.



## FUTURE SCOPE

**Approach to Spin-Polarized Magnetic Wire**

Since the strategy for spin-alignment of localized spins on  $\pi$ -radical units through spin-polarized conduction electrons has been established, one may design a ferromagnetic molecular wire which pass a spin-polarized current along a  $\pi$ -conjugating polymer carrying  $\pi$ -radical units as pendant groups. A hole-doped polypyrrole is known to exhibit a high conductivity on the basis of the polaronic mechanism. If a pyrrole-based spin-polarized donor is used as a building block of the conducting polymer, the electron which can be transmitted along the chain is spin-polarized to  $\uparrow$ , aligning all the localized spins on the pendant groups to  $\uparrow$ .<sup>30</sup> Such a spin-polarized magnetic wire must become an indispensable part of a quantum spin device.

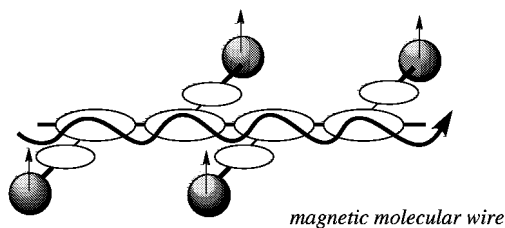


**Figure 26.** Magnetic molecular wire composed of spin-polarized donors.

## REFERENCES

1. a) Tour, J.M. (1996). *Chem. Rev.*, **96**, 537-553; b) Moore, J.S. (1997). *Acc. Chem. Res.*, **30**, 402-413; c) Morgenroth, F.M., Kübel, C., Müllen, K. (1997). *J. Mater. Chem.*, **7**, 1207-1211; d) Roncali, J. (1997). *J. Mater. Chem.*, **7**, 2307-2321; e) Bryce, M.R., Devonport, W., Goldenberg, L.M., Wang, C. (1998). *Chem. Commun.*, 945-951; f) Nakanishi, H., Sumi, N., Aso, Y., Otsubo, T. (1998). *J. Org. Chem.*, **63**, 8632-8633.
2. Yamamoto, T. (1999). *Bull. Chem. Soc. Jpn.*, **72**, 621-638.
3. a) Itoh, K. (1967). *Chem. Phys. Lett.*, **1**, 235; b) Wasserman, E., Murray, R.W., Yanger, W.A., Trozzolo, A.M. and Smolinsky, G. (1967). *J. Am. Chem. Soc.*, **89**, 5076; c) Sugawara, T., Bandow, S., Kimura, K., Iwamura, H. and Itoh, K. (1984). *J. Am. Chem. Soc.*, **106**, 6449; d) Sugawara, T., Bandow, S., Kimura, K., Iwamura, H. and Itoh, K. (1986). *J. Am. Chem. Soc.*, **108**, 368.
4. a) Rajca, A., Lu, K. and Rajca, S. (1997). *J. Am. Chem. Soc.*, **119**, 10335-10345; b) Rajca, A., Rajca, S. and Wongsriratanakul, J. (1999). *J. Am. Chem. Soc.*, **121**, 6308-6309; c) Matsuda, K., Nakamura, N., Inoue, K., Koga, N. and Iwamura, H. (1996). *Bull. Chem. Soc. Jpn.*, **69**, 1483-1494; d) Murray, M.M., Kaszynski, P., Kaisaki, D.A., Chang, W. and Dougherty, D.A. (1994). *J. Am. Chem. Soc.*, **116**, 8152-8161; e) Nakazaki, J., Matsushita, M.M., Izuoka, A. and Sugawara, T. (1997). *Mol. Cryst. Liq. Cryst.*, **306**, 81-88; f) Wienk, M.M. and Janssen, R.A.J. (1997). *J. Am. Chem. Soc.*, **119**, 4492-4501; g) Stickley, K.R., Selby, T.D. and Blackstock, S.C. (1997). *J. Org. Chem.*, **62**, 448-449; h) Sato, T., Hori, K. and Tanaka, K. (1998). *J.*

- Mater. Chem.*, **8**, 589-593; i) Bushby, R.J. and Gooding, D. (1998). *J. Chem. Soc. Perkin Trans. 2*, 1069-1075; j) Nishide, H., Kaneko, T., Nii, T., Katoh, K., Tsuchida, E. and Lahti, P.M. (1996). *J. Am. Chem. Soc.*, **118**, 9695-9704; k) Nishide, H., Miyasaka, M. and Tsuchida, E. (1998). *Angew. Chem. Int. Ed.*, **37**, 2400-2402; l) Yamamoto, T. and Hayashi, H. (1997). *J. Polym. Sci. A*, **35**, 463-474; m) Oka, H., Tamura, T., Miura, Y. and Teki, Y. (1999). *J. Mater. Chem.*, **9**, 1227-1232; n) Xie, C. and Lahti, P.M. (1999). *J. Polym. Sci. A*, **37**, 779-788.
5. a) Ishiguro, K., Ozaki, M., Sekine, N. and Sawaki, Y. (1997). *J. Am. Chem. Soc.*, **119**, 3625-3626; b) Hamachi, K., Matsuda, K. and Iwamura, H. (1998). *Bull. Chem. Soc. Jpn.*, **71**, 2937-2943; c) Matsuda, K. and Irie, M. (2000). *Chem. Lett.*, 16-17.
  6. a) Kumai, R., Sakurai, H., Izuoka, A. and Sugawara, T. (1996). *Mol. Cryst. Liq. Cryst.*, **279**, 133-138; b) Sakurai, H., Kumai, R., Izuoka, A. and Sugawara, T. (1996). *Chem. Lett.*, 879-880; c) Sugawara T. (1999). *Mol. Cryst. Liq. Cryst.*, **334**, 257-273; d) Izuoka, A., Hiraiishi, M., Abe, T., Sugawara, T., Sato, K. and Takui, T. (2000). *J. Am. Chem. Soc.*, **122**, 3234-3235.
  7. a) Izuoka, A., Kumai, R. and Sugawara, T. (1995). *Adv. Mater.*, **7**, 672-674; b) Sugawara, T. and Izuoka, A. (1997). *Mol. Cryst. Liq. Cryst.*, **305**, 41.
  8. McConnell, H.M. (1963). *J. Chem. Phys.*, **39**, 1910.
  9. a) Izuoka, A., Murata, S., Sugawara, T. and Iwamura, H. (1985). *J. Am. Chem. Soc.*, **107**, 1786-1787; b) Izuoka, A., Murata, S., Sugawara, T. and Iwamura, H. (1987). *J. Am. Chem. Soc.*, **109**, 2631-2639.
  10. Sugawara, T., Tukada, H., Izuoka, A., Murata, S. and Iwamura H. (1986). *J. Am. Chem. Soc.*, **108**, 4272-4278.
  11. Sugawara, T., Murata, S., Kimura, K., Iwamura, H., Sugawara, Y. and Iwasaki, H. (1985). *J. Am. Chem. Soc.*, **107**, 5293-5294.
  12. a) Duffly, W. Jr., Strandburg, D.L. and Deck, J.F. (1969). *Phys. Rev.*, **183**, 567; b) Takizawa, O. (1976). *Bull. Chem. Soc. Jpn.*, **49**, 583.
  13. Sugawara, T., Izuoka, A., Murata, S. and Iwamura, H. (1988). *Mol. Cryst. Liq. Cryst.*, **154**, 345-350.
  14. a) Izuoka, A., Fukada, M., Sugawara, T., Sakai, M. and Bandow, S. (1992). *Chem. Lett.*, 1627-1630; b) Izuoka, A., Fukada, M., Kumai, R., Itakura, M., Hikami, S. and Sugawara, T. (1994). *J. Am. Chem. Soc.*, **116**, 2609-2610; c) Nishizawa, M., Shiomi, D., Sato, K., Takui, T., Itoh, K., Sawa, H., Kato, R., Sakurai, H., Izuoka, A. and Sugawara, T. (2000). *J. Chem. Phys. B*, **104**, 503-509.
  15. a) Nogami, T., Tomioka, K., Ishida, T., Yoshikawa, H., Yasui, M., Iwasaki, F., Iwamura, H., Takeda, N. and Ishikawa, M. (1994). *Chem. Lett.*, 29-32; b) Nogami, T., Ishida, T., Yasui, M., Iwasaki, F., Takeda, N., Ishikawa, M., Kawakami, T. and Yamaguchi, K. (1996). *Bull. Chem. Soc. Jpn.*, **69**, 1841-1848; c) Togashi, K., Imachi, R., Tomioka, K., Tsuboi, H., Ishida, T., Nogami, T., Takeda, N. and Ishikawa, M. (1996). *Bull. Chem. Soc. Jpn.*, **69**, 2821-2830.
  16. Chiarelli, R., Novak, M.A., Rassat, A. and Tholence, J.L. (1993). *Nature*, **363**, 147-149.
  17. a) Mukai, K., Konishi, K., Nedachi, K. and Takeda, K. (1995). *J. Magn. Magn. Mater.*, **140-144**, 1449-1450; b) Mukai, K., Nuwa, M., Morishita, T., Muramatsu, T., Kobayashi, T.C. and Amaya, K. (1997). *Chem. Phys. Lett.*, **272**, 501-505; c) Mukai, K., Nuwa, M., Suzuki, K., Nagaoka, S., Achiwa, N. and Jamali, J.B. (1998). *J. Phys. Chem. B*, **102**, 782-787.
  18. a) Kinoshita, M., Turek, P., Tamura, M., Nozawa, K., Shiomi, D., Nakazawa, Y., Ishikawa, M., Takahashi, M., Awaga, K., Inabe, T. and Maruyama, Y. (1991). *Chem. Lett.* 1225-1228; b) Tamura, M., Nakazawa, Y., Shiomi, D., Nozawa, K., Hosokoshi, Y., Ishikawa, M., Takahashi, M. and Kinoshita, M. (1991). *Chem. Phys. Lett.*, **186**, 401-404.
  19. [PNPN neutron mSR]
  20. Kumai, R., Matsushita, M.M., Izuoka, A. and Sugawara, T. (1994). *J. Am. Chem. Soc.*, **116**, 4523-4524.
  21. a) Sugawara, T., Matsushita, M.M., Izuoka, A., Wada, N., Takeda, N. and Ishikawa, M. (1994). *J. Chem. Soc., Chem. Commun.*, 1723-1724; b) Matsushita, M.M., Izuoka, A., Sugawara, T., Kobayashi, T., Wada, N., Takeda, N. and Ishikawa, M. (1997). *J. Am. Chem. Soc.*, **119**,

- 4369-4379.
22. a) Ishiguro, K., Ozaki, M., Kamekura, Y., Sekine, N., Sawaki, Y., (1997). *Mol. Cryst. Liq. Cryst.*, **306**, 75-80; b) Ishiguro, K., Ozaki, M., Sekine, N., and Sawaki, Y. (1997). *J. Am. Chem. Soc.*, **119**, 3625-3626.
  23. Maruda, G., Takeda, S., Matsushita, M.M., Izuoka, A., Sugawara, T., Yamaguchi, K., (1997). Symposium on Molecular Structure, Fukuoka, Japan, Abstr. 4E02, p640.
  24. Oda, A., Kawakami, T., Takeda, S., Mori, W., Matsushita, M.M., Izuoka, A., Sugawara, T., Yamaguchi, K., (1997) *Mol. Cryst. Liq. Cryst.*, **306** 151-160.
  25. a) Cirujeda, J., Mas, M., Molins, E., Panthou, F.L., Laugier, J., Park, J.G., Paulsen, C., Rey, P., Rovira, C. and Veciana, J. (1995). *J. Chem. Soc., Chem. Commun.*, 709-710; b) Caneschi, A., Ferraro, F., Gatteschi, D., Lirzin, A., Novak, M.A., Rentschler, E. and Sessoli, R. (1995). *Adv. Mater.*, **7**, 476-478.
  26. a) Sugawara, T. (1989). *J. Synth. Org. Chem. Jpn.*, **47**, 306-320; b) Yamaguchi, K., Namimoto, H., Fueno, T., Nogami, T. and Shirota, Y. (1990). *Chem. Phys. Lett.*, **166**, 408-414; c) Izuoka, A., Kumai, R., Tachikawa, T. and Sugawara, T. (1992). *Mol. Cryst. Liq. Cryst.*, **218**, 213-218.
  27. a) Kumai, R., Izuoka, A. and Sugawara, T. (1993). *Mol. Cryst. Liq. Cryst.*, **232**, 151-154; b) Kumai, R., Matsushita, M.M., Izuoka, A. and Sugawara, T. (1994). *J. Am. Chem. Soc.*, **116**, 4523-4524.
  28. Nakazaki, J., Matsushita, M.M., Izuoka, A. and Sugawara, T. (1999). *Tetrahedron Lett.*, **40**, 5027-5030.
  29. Nakazaki, J., Ishikawa, Y., Izuoka, A., Sugawara, T. and Kawada, Y. (2000). *Chem. Phys. Lett.*, **319**, 385-390.
  30. Nakazaki, J., Matsushita, M.M., Izuoka, A. and Sugawara, T. (1997). *Mol. Cryst. Liq. Cryst.*, **306**, 81-88.